SLAC-PUB-8515
July 2000

Beamline Model Verification Using Model Independent Analysis

J. Irwin and Y. T. Yan

Invited talk presented at the Seventh European Particle Accelerator,
6/26/2000—6/26/2000, Vienna, Austria

Stanford Linear Accelerator Center, Stanford University, Stanford, CA 94309

Work supported by Department of Energy contract DE–AC03–76SF00515.

BEAMLINE MODEL VERIFICATION USING MODEL INDEPENDENT ANALYSIS *

J. Irwin and Y.T. Yan, SLAC, Stanford, CA 94309, U.S.A.

Abstract

Model Independent Analysis (MIA) has previously employed statistical methods to reveal sub-resolution correlated modes present in pulse-by-pulse beam-position-monitor (BPM) measurements at the SLAC linac [1]. This paper describes an extension of MIA to verify local linear and nonlinear properties of linac and storage ring lattices. Measurements and analysis of the LER ring at PEP-II are presented as an example.

1 INTRODUCTION

To utilize precision beam measurements to verify a beamline model one must identify and remove relatively large variations in BPM offsets, gains, cross-plane couplings, and nonlinear pin-cushion distortions. In section 2 it is proven that all such BPM attributes may be represented by symplectic maps. In section 3 it is shown that given the orbit data for four independent excitations of a beamline one can use symplectic methods to extract the four Green's functions between BPM outputs. In the linear case the Green's functions are specified by values for R_{12}, R_{14}, R_{32}, and R_{34}. Section 4 establishes that even in the case of single-view BPMs this is sufficient information to identify the gain and cross-plane-coupling BPM errors as well as one normal and one skew attribute of the linear lattice between each BPM pair. In the case of double-view BPMs there is sufficient information to determine two normal and two skew lattice attributes. Section 5 describes the use of MIA to extract precision excitation modes from observations of a shaken beam in a storage ring, and section 6 presents a first attempt to use this method to verify the lattice of the low-energy ring (LER) of PEP-II. In section 7 it is shown how these methods may be extended to determine nonlinear BPM errors and nonlinear lattice parameters.

2 SYMPLECTIC BPM-ERROR MAPS

2.1 Linear errors

The BPM offsets may be removed by observing, and later subtracting, the average BPM measurement during unexcited operation. Assuming that a change in the beam's slope at a BPM does not effect its output, the linear errors can be represented by four numbers: the horizontal and vertical gain, g_x and g_y, the change in the horizontal output from a vertical beam displacement, θ_{xy}, and the change in the vertical output from a horizontal beam displacement, θ_{yx}. This information can be placed in a 4x4 symplectic matrix:

$$G = \begin{pmatrix} G & 0 \\ 0 & {G^{-1}}^T \end{pmatrix} \text{ with } G = \begin{pmatrix} g_x & \theta_{xy} \\ \theta_{yx} & g_y \end{pmatrix} ,$$

where the symplectic identity is given by

$$J = \begin{pmatrix} 0 & I \\ -I & 0 \end{pmatrix} .$$

2.2 Nonlinear errors

Assuming that nonlinear distortions do not depend on beam slope, they will have Lie generators of the form $g = -x' f_x(x,y) - y' f_y(x,y)$, producing $\Delta x(x,y) = f_x(x,y) + ...$ and $\Delta y(x,y) = f_y(x,y) + ...$. Any nonlinear shape can be produced. The map output for x' and y' is irrelevant because these are not measured.

3 LINEAR GREEN'S FUNCTIONS

The previous section implies that maps between BPM outputs can be assumed symplectic, being the composition of 3 symplectic maps: the inverse of the map from the beginning of the lattice section to the initial BPM output, the map through the lattice section, and the map from the end of the lattice section to the final BPM output.

Suppose one has the BPM measurements for 4 linear independent modes of a beamline. Though x' and y' are not measured they exist, and at the a^{th} and b^{th} BPM output one could conceptually form a matrix consisting of the phase-space coordinates for the four independent excitations: eg.

$$Z^a = \begin{pmatrix} x_1^a & x_2^a & x_3^a & x_4^a \\ x_1'^a & x_2'^a & x_3'^a & x_4'^a \\ y_1^a & y_2^a & y_3^a & y_4^a \\ y_1'^a & y_2'^a & y_3'^a & y_4'^a \end{pmatrix} .$$

Since the phase-space coordinates at a and b are related by a symplectic map, R^{ba}, one has $Z^b = R^{ba} Z^a$. The symplecticity of R means ${R^{ba}}^T J R^{ba} = J$, and it follows that the anti-symmetric matrix $Q = {Z^b}^T J Z^b = {Z^a}^T J Z^a$ is a constant around the ring, even in a strongly coupled lattice. The 6 independent elements of Q are the generalization of the Wronskian in 1 d.o.f. Since Z^a has an inverse (the 4 modes are independent), left-multiply the expression for Q by ${Z^a}^{T\,-1}$, right-multiply by ${Z^a}^{-1}$ and invert to get $Z^a Q^{-1} {Z^a}^T = -J$, where Q^{-1} is an anti-symmetric matrix whose elements are a permutation of the elements of Q divided by its determinant.

* Work supported by DOE contract DE-AC03-76SF00515.

Now suppose there are horizontal-view BPMs at a and c and vertical-view BPMs at b and d. Define 4x4 matrices that contain the modes as measured at these BPMs and contain the map elements from a to the other locations.

$$\hat{Z} = \begin{pmatrix} x_1^a & x_2^a & x_3^a & x_4^a \\ y_1^b & y_2^b & y_3^b & y_4^b \\ x_1^c & x_2^c & x_3^c & x_4^c \\ y_1^d & y_2^d & y_3^d & y_4^d \end{pmatrix} ,$$

$$\hat{R} = \begin{pmatrix} 1 & 0 & 0 & 0 \\ R_{31}^{ba} & R_{32}^{ba} & R_{33}^{ba} & R_{34}^{ba} \\ R_{11}^{ca} & R_{12}^{ca} & R_{13}^{ca} & R_{14}^{ca} \\ R_{31}^{da} & R_{32}^{da} & R_{33}^{da} & R_{34}^{da} \end{pmatrix} .$$

Then $\hat{Z} = \hat{R}Z^a$. Pre-multiplying $Z^a Q^{-1} {Z^a}^T = -J$ by $\hat{R}$, and post-multiplying by $\hat{R}^T$ yields $\hat{Z}Q^{-1}\hat{Z}^T = -\hat{R}J\hat{R}^T$.

The elements of $\hat{R}J\hat{R}^T$ are Green's function elements of the various maps between a, b, c and d, and the components of this matrix equation have the extremely simple form

$$\sum_{i<j} (x_i^a y_j^b - x_j^a y_i^b) Q_{ij}^{-1} = R_{lm}^{ba} . \qquad (1)$$

The RHS is always a Green's function element ($R_{12}, R_{32}, R_{14},$ or R_{34}); the first index, l is 1 or 3 according to whether "b" is horizontal or vertical, and the second index, m is 2 or 4 according to whether "a" is horizontal or vertical. Note that in this equation for R^{ba} only measurements at a and b enter; what's happening at c and d is actually irrelevant. The amplitude and orthogonality of the 4 modes being used enters through Q. The result in eq. (1) is a tidy expression for the local linear Green's function matrix elements between any two locations in the beamline.

4 VERIFYING THE LINEAR MODEL

Not all of these Green's function equations can be independent. Since there are 4 measurements at each single-view BPM, 1 for each of the 4 modes, one might expect each BPM to be involved in 4 independent equations. Except for BPMs at the end and beginning of a beamline, this is indeed true: there are 2 independent "normal" measurements and 2 independent "skew" measurements. For double-view BPMs one expects eight relationships. One can show that all Green's function elements may be expressed in terms of elements between neighbors and next-nearest neighbors. For example, for J as above, and "B" the Green's function sub-matrix of

$$R = \begin{pmatrix} A & B \\ C & D \end{pmatrix} ,$$

then, $B^{da} = B^{db} {B^{cb}}^{-1} B^{ca} - B^{dc} {B^{cb}}^{T^{-1}} B^{ba}$, where a, b, c and d are four consecutive double-view BPMs.

The introduction of an additional single-view BPM implies the introduction of an unknown normal gain and an unknown skew cross-plane coupling. Since there are four new equations, there remain two relationships that can be used to verify the lattice. Typically one has a BPM at every main quadrupole or half-cell. If there is a sextupole in this half-cell, then the equations can determine the horizontal and vertical position of the sextupole, relative to the beam. In other words, since in addition to determining BPM parameters, we typically have only 2 (or 4) relationships per beamline interval, we can not determine the 6 possible parameters of an arbitrary symplectic map. However, many properties of the beamline interval are not in doubt, such as the longitudinal position of elements and individual strengths of elements on strings. One makes the most of such information, limiting the unknowns to less than one normal and one skew parameter per BPM in the case of single-view, or two normal and two skew parameters in the case of double-view BPMs.

5 OBTAINING MODES IN RINGS

In linacs there is often enough incoming jitter in the beam to measure and identify betatron modes. In rings this is usually not the case, and one must introduce excitation. Shakers are typically used to measure tunes. In PEP-II it is relatively easy to shake the beam to amplitudes of a few mm. Since the BPM resolution is a few μms one obtains information with parts per thousand accuracy potential. The beam profile does not seem to be noticeably altered by shaking, so one avoids the decoherence inherent in enlarged beams. To obtain these amplitudes, one must shake at a frequency close to the betatron frequency. Thus the horizontal shaker and vertical shaker must operate at different frequencies. To determine higher order information, it is necessary to have enhanced horizontal and vertical amplitudes simultaneously. Having collected data from many consecutive turns for an ensemble of BPMs, an SVD analysis is used to identify correlated modes. Typically 2 betatron modes in the shaken plane are very large and all other modes are close to the noise floor. The eigenvalues of these other modes may be set to zero, and the SVD decomposition re-multiplied to obtain a noise-reduced data matrix. A linear portion of the lattice can now be decomposed in an SVD product, to identify the initial amplitude of the two betatron modes on each turn. These amplitudes can be further filtered using a hypothesis on the form of the turn-to-turn map. One obtains highly refined initial amplitude data. These initial amplitudes and their products can now be used in conjunction with the original data matrix to project out high quality eigenmodes (resolution now going as $\sqrt{P}$, the number of pulses). Thus one obtains response vectors around the ring to any amplitude product. The local values of these vectors are precisely the coefficients of the one-turn map from the linear starting region to each BPM location. They may be used to determine the linear and nonlinear local Green's functions.

6 APPLICATION TO PEP-II

We have tried some preliminary applications of least square fitting of Eq. 1 to the PEP-II Low Energy Ring (LER) in order to find magnet errors. The fitting variables are the BPM errors and the magnet errors by inserting, at each location of the quadrupole or the sextupole (for misalignment), a varying normal quad and a varying skew quad. Since most of the PEP-II BPMs are single-view BPMs, in order that BPM errors can also be part of the fitting, we make a modification of Eq. 1 by transforming it into the measurement frame such that the LHS is kept the same and the x's and y's stand for the measured coordinates which include BPMs error effect while the RHS is modified such that R_{12}, R_{32}, R_{14}, and R_{34} are replaced with $\mathcal{R}_{12}, \mathcal{R}_{32}, \mathcal{R}_{14}$, and $\mathcal{R}_{34}$, where

$$\mathcal{R}_{12} = g_x^b R_{12} g_x^a + g_x^b R_{14} \theta_{xy}^a + \theta_{xy}^b R_{32} g_x^a + \theta_{xy}^b R_{34} \theta_{xy}^a,$$

$$\mathcal{R}_{32} = g_y^b R_{32} g_x^a + g_y^b R_{34} \theta_{xy}^a + \theta_{yx}^b R_{12} g_x^a + \theta_{yx}^b R_{14} \theta_{xy}^a,$$

$$\mathcal{R}_{14} = g_x^b R_{14} g_y^a + g_x^b R_{12} \theta_{yx}^a + \theta_{xy}^b R_{34} g_y^a + \theta_{xy}^b R_{32} \theta_{yx}^a,$$

$$\mathcal{R}_{34} = g_y^b R_{34} g_y^a + g_y^b R_{32} \theta_{yx}^a + \theta_{yx}^b R_{14} g_y^a + \theta_{yx}^b R_{12} \theta_{ya}^a.$$

The first step we do is to get the 4 independent orbits and calculate the invariants so that the LHS of Eq. 1 can be calculated. We would get 2 sets (x data and y data) of about 2000 turns of orbit data for all BPMs from excitation of horizontal (x) motion and another 2 sets of about 2000 turns of orbit data from excitation of vertical (y) motion. We then perform Fourier transformation (if necessary) to cut the low-frequency noise and then the singular value decomposition (SVD) to get the 2 betatron modes (the largest two modes) for each of the 4 sets of data to form the 4 independent orbits.

The second step we do is to get the local transfer matrices and then insert a matrix of the form

$$\begin{pmatrix} 1 & 0 & 0 & 0 \\ q_n & 1 & q_s & 0 \\ 0 & 0 & 1 & 0 \\ q_s & 0 & -q_n & 1 \end{pmatrix}$$

at each quadrupole or sextupole location, where q_n and q_s are variables representing the normal and skew quad errors to be fitted. Besides the constraints from Eq. 1, we further impose constraints that require g_x's and g_y's to be close to 1 and θ_{xy} and θ_{yx} to be close to 0 for all BPMs in the least square fitting (note that we have removed the bad BPMs during the process of getting the 4 independent orbits).

Figure 1 shows a fitted results from simulation (orbit data obtained from numerical trackings) with 5 magnet errors purposely imposed for a portion (covering 21 BPMs) of the arc section after the injection. The BPM errors are randomly generated. The top plot shows that the magnet errors (normal quad or skew quad errors) are fitted pretty well even though the BPM errors, particularly the coupled errors θ_{xy} and θ_{yx}, are not perfectly fitted, as shown on the bottom plots, due that the invariants are not calculated accurately.

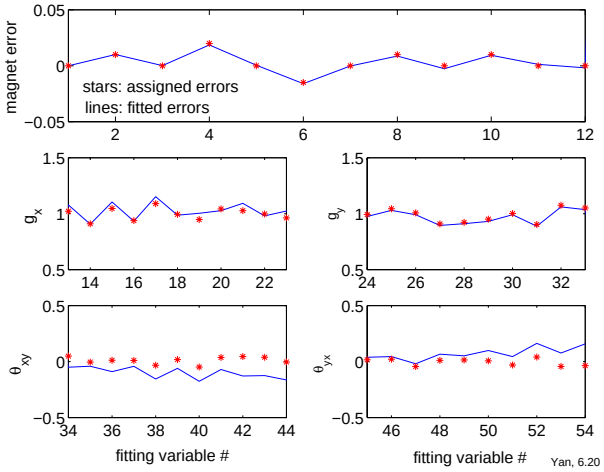

Figure 1: Magnet error fitting for PEP-II LER. The orbit data are obtained from computer particle tracking.

Figure 2 shows the fitted results from measurement (orbit data obtained from buffered data acquisition of the PEP-II LER machine) for $\mathcal{R}_{12}$ (top) and $\mathcal{R}_{34}$ (bottom) in the measurement frame for the same arc section as in Fig. 1. Note that in the arc section, although the local R_{12}'s are the same (a constant) and so do the local R_{34}'s, the modified $\mathcal{R}_{12}$'s and $\mathcal{R}_{34}$'s in the measurement frame include the BPM errors and so are not constants.

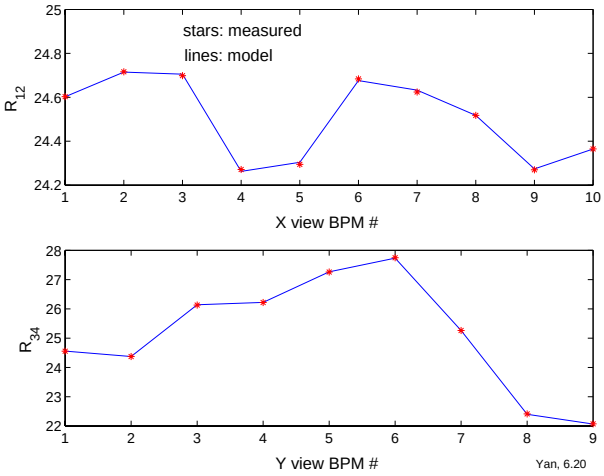

Figure 2: Magnet error fitting for PEP-II LER. The orbit data are obtained from buffered data acquisition of the LER machine.

7 NONLINEARITIES

The result of the MIA orbit determination may be written

$$\vec{b}(z) = \sum_{\vec{n}} \vec{v}_{\vec{n}} z^{\vec{n}}$$

and $z^{\vec{n}} = x^{n_x} x'^{n_{x'}} y^{n_y} y'^{n_{y'}}$, where $\vec{b}$ is the vector of BPM readings around the ring, $\vec{v}_{\vec{n}}$ are the values of the n^{th} mode around the ring, and $z^{\vec{n}}$ is the amplitude on any given pulse of the $\vec{n}^{th}$ mode. For the linear case only the 1^{st} order terms are retained, and the four linear $\vec{v}s$ are the values of the four modes used in section 3 to deduce eq. 1 for the local Green's functions. To deduce the nonlinear Greens function, replace z by $z_o + \zeta$, where z_o is assumed small, and ζ is an infinitesimal that is retained to first order only.

$$\vec{b}(z_o + \zeta) = \vec{b}(z_o) + \sum_k \frac{\partial \vec{b}}{\partial z_k}(z_o)\zeta_k.$$

Looking at this expression as a function of ζ the form is similar to the linear case with modes

$$\vec{v}_k(z_o) = \frac{\partial \vec{b}}{\partial z_k}(z_o).$$

By stepwise adding terms of higher order one can determine each of the higher order contributions to the Green's function. To illustrate how this works consider the 2^{nd}-order terms for a single variable. In addition to the constant term, $\vec{v}_k(z_o)$ will have linear terms in x_o and x'_o. Using Eq. 1 these linear terms contribute terms to the local Green's function linear in x_o and x'_o.

On the other hand, the local map has the form:

$$x^b = R^{ba}_{11}x^a + R^{ba}_{12}x'^a + R^{ba}_{111}x^{a\,2} + R^{ba}_{112}x^a x'^a + R^{ba}_{122}x'^{a\,2}.$$

Taking the derivative with respect to x' gives the Green's function

$$\frac{\partial x^b}{\partial x'^a} = R^{ba}_{12} + R^{ba}_{112}x^a + 2R^{ba}_{122}x'^a.$$

Assuming that the linear lattice was successfully verified, the values of x^a and x'^a are determined as linear combination of x_o and x'_o. The two coefficients R_{112} and R_{122} are determined by comparison with the 2 new contributions to the Green's function.

8 ACKNOWLEDGEMENT

We thank T. Hilmel and M. Minty for help in PEP-II data acquisition and Y. Cai for helpful discussions.

9 REFERENCES

[1] J. Irwin, C.X. Wang, Y. Yan, et. al., "Model-Independent Beam Dynamics Analysis," Phys. Rev. Lett. **82**, 1684 (1999).